0026-895X/01/5904-825–836$3.00
MOLECULAR PHARMACOLOGY
Copyright © 2001 The American Society for Pharmacology and Experimental Therapeutics
Mol Pharmacol 59:825–836, 2001

Vol. 59, No. 4
456/891509
Printed in U.S.A.

Direct Effects of Candesartan and Eprosartan on Human Cloned Potassium Channels Involved in Cardiac Repolarization

RICARDO CABALLERO, EVA DELPÓN, CARMEN VALENZUELA, MÓNICA LONGOBARDO, TERESA GONZÁLEZ, and JUAN TAMARGO

Department of Pharmacology, School of Medicine, Universidad Complutense, Madrid, Spain

Received July 31, 2000; accepted December 22, 2000

This paper is available online at http://molpharm.aspetjournals.org

ABSTRACT

In the present study, we analyzed the effects of two angiotensin II type 1 receptor antagonists, candesartan (0.1 μM) and eprosartan (1 μM), on hKv1.5, HERG, KvLQT1+minK, and Kv4.3 channels expressed on *Ltk*$^-$ or Chinese hamster ovary cells using the patch-clamp technique. Candesartan and eprosartan produced a voltage-dependent block of hKv1.5 channels decreasing the current at +60 mV by 20.9 ± 2.3% and 14.3 ± 1.5%, respectively. The blockade was frequency-dependent, suggesting an open-channel interaction. Eprosartan inhibited the tail amplitude of HERG currents elicited on repolarization after pulses to +60 mV from 239 ± 78 to 179 ± 72 pA. Candesartan shifted the activation curve of HERG channels in the hyperpolarizing direction, thus increasing the current amplitude elicited by depolarizations to potentials between −50 and 0 mV. Candesartan reduced the KvLQT1+minK currents elicited by 2-s pulses to +60 mV (38.7 ± 6.3%). In contrast, eprosartan transiently increased (8.8 ± 2.7%) and thereafter reduced the KvLQT1+minK current amplitude by 17.7 ± 3.0%. Eprosartan, but not candesartan, blocked Kv4.3 channels in a voltage-dependent manner (22.2 ± 3.5% at +50 mV) without modifying the voltage-dependence of Kv4.3 channel inactivation. Candesartan slightly prolonged the action potential duration recorded in guinea pig papillary muscles at all driving rates. Eprosartan prolonged the action potential duration in muscles driven at 0.1 to 1 Hz, but it shortened this parameter at faster rates (2–3 Hz). All these results demonstrated that candesartan and eprosartan exert direct effects on Kv1.5, HERG, KvLQT1+minK, and Kv4.3 currents involved in human cardiac repolarization.

Angiotensin II plays an important role in maintaining blood pressure and sodium and water homeostasis; most of its effects are mediated by the type 1 receptor (AT_1) (Timmermans et al., 1993). Thus, the specific, nonpeptide, orally active AT_1 receptor antagonists are the newest drug class to become available for the treatment of hypertension (Burnier and Brunner, 2000). Candesartan and eprosartan are AT_1 antagonists that produce a different type of blockade because of their different structure (Unger, 1999). The candesartan AT_1 binding affinity is 80 times greater than that of losartan and in functional and ligand binding experiments produces a long-lasting competitive antagonism because of its very slow dissociation rate from the AT_1 receptor (Sever and Holzgreve, 1997). Eprosartan exhibits also a high affinity for the AT_1 receptor and produces a competitive antagonism (McClellan and Balfour, 1998).

Candesartan has been described to decrease the incidence of reperfusion arrhythmias in mice, which suggested that angiotensin II is involved in the genesis of ventricular arrhythmias through AT_1 receptors (Harada et al., 1998). Furthermore, candesartan inhibited the shortening of the atrial effective refractory period induced by rapid pacing, thus preventing the electrical remodeling produced by atrial fibrillation in dogs (Nakashima et al., 2000). These antiarrhythmic actions of candesartan could be the consequence of AT_1 receptor blockade and/or direct effects of the drug on ion currents involved in cardiac repolarization. Candesartan does not modify inward calcium current in sinoatrial node cells of rabbits (Habuchi et al., 1995), but its effects on cardiac Na^+ and K^+ channels have been unknown until now. Both in healthy volunteers and in hypertensive patients, candesartan (Hubner et al., 1997; McClellan and Goa, 1998) and eprosartan (McClellan and Balfour, 1998) produce no significant changes on the surface electrocardiogram, even when the effects of both drugs on QT dispersion and ventricular refractoriness are unknown.

Several voltage-dependent outward K^+ currents play a critical role in repolarization and determine the duration of

Supported by Grants SAF-99-0069, CAM 08.4/0016/1998, and SAF98-0058.

ABBREVIATIONS: AT_1, Angiotensin II type 1 receptor; I_{Kur}, ultrarapid delayed rectifier current; I_{Kr}, the rapid component of the delayed rectifier current; I_{Ks}, the slow component of the delayed rectifier current; HERG, human ether-a-go-go-related gene; CHO, Chinese hamster ovary cells; $[K^+]_i$, intracellular K^+ concentration; K_D, apparent affinity constant; I-V, current-voltage relationship; APD, action potential duration, *K*, rate constant of the onset kinetics of frequency-dependent block.

the human cardiac action potential including: 1) the transient outward current, 2) the rapidly activating slowly inactivating delayed rectifier current (I_{Kur}), and 3) the fast (I_{Kr}) and slow (I_{Ks}) components of the delayed rectifier current (Roden and George, 1997). Recent data suggest that Kv4.3 α-subunits might underlie the 4-aminopyridine sensitive component of transient outward current (I_{to1}) in human myocytes (Dixon et al., 1996; Wang et al., 1999). The *Shaker*-related hKv1.5 channel has been cloned from human ventricle (Tamkun et al., 1991), and has been identified as the counterpart of the I_{Kur} described in human atrial myocytes (Wang et al., 1993). Expression of HERG, identified as the locus of congenital long QT syndrome type 2 mutations, reveals inwardly rectifying K^+ currents similar to I_{Kr}, suggesting that HERG underlies cardiac I_{Kr} (Sanguinetti et al., 1995), even when functional I_{Kr} channels result from the coassembly of HERG α-subunits and MinK-related peptide β-subunits (Abbott et al., 1999). Finally, coassembly of KvLQT1 α-subunits with minK β-subunits forms the channels underlying I_{Ks} currents (Barhanin et al., 1996; Sanguinetti et al., 1996).

Very recently, it has been described that losartan, the prototype of the AT_1 receptor antagonists and its active metabolite, E3174, at clinically relevant concentrations, directly modified delayed rectifier K^+ currents involved in human cardiac repolarization. Losartan inhibited hKv1.5, HERG and I_{Ks} currents, whereas E3174 inhibited hKv1.5 and I_{Ks} and increased HERG currents. Moreover, these actions were correlated with modifications on the action potential duration (Caballero et al., 2000). These findings suggested that the AT_1 receptor antagonists may exert different effects on K^+ currents responsible for repolarization. Therefore, the present study was undertaken to analyze the direct effects of candesartan and eprosartan, on hKv1.5, HERG, and KvLQT1+minK channels cloned from human heart and on Kv4.3 channels cloned from rat heart and expressed in mammalian cell lines and the possible consequences of their effects on the action potentials recorded in guinea pig papillary muscles. The results indicated that candesartan and eprosartan modified hKv1.5, HERG, KvLQT1+minK, and Kv4.3 channels in a time- and voltage-dependent manner. Moreover, candesartan slightly lengthened the action potential duration in a frequency-independent manner, whereas eprosartan produced a reverse use-dependent prolongation.

Materials and Methods

Transmembrane Action Potentials. Transmembrane action potentials were recorded in guinea pig (250–300 g) papillary muscles (2–3 mm long and less than 1 mm in diameter) through glass microelectrodes filled with 3 M KCl (tip resistance, 8–15 MΩ) using procedures described previously (Pérez et al., 1997). The microelectrode was connected via Ag-AgCl wire to high-input impedance, capacity-neutralizing amplifiers (model 701; WPI, New Haven, CT). Driving stimuli were rectangular pulses (1–2 ms in duration) delivered from a multipurpose programmable stimulator (CS-220; Cibertec SA, Madrid, Spain). Action potentials were displayed on an oscilloscope and stored in a Hewlett-Packard computer by use of Cibertec software. The following parameters of the transmembrane action potential were measured: resting membrane potential, amplitude and action potential duration at the 50% (APD_{50}) and 90% (APD_{90}) level of repolarization. The preparations were initially driven at 1 Hz and a period of 1 h was allowed for equilibration, during which a stable impalement was obtained. After equilibration period, the effects of 0.1 μM candesartan or 1 μM eprosartan on values for amplitude and action potential duration at 50% and 90% at steady state were studied in muscles stimulated at different driving rates (0.1–3 Hz).

Cell Culture. Cell culture of *Ltk* cells stably expressing hKv1.5 channels has been described in detail elsewhere (Snyders et al., 1993; Caballero et al., 1999; Delpón et al., 1999). Transfected cells were cultured in Dulbecco's modified Eagle's medium (Sigma Chemical Co. London, UK) supplemented with 10% horse serum and 0.25 mg/ml G418 (a neomycin analog; Life Technologies, Grand Island, NY) in a 5% CO_2 atmosphere. Before experimental use, subconfluent cultures were incubated with 2 μM dexamethasone for 24 h as expression of the channel was under control of a dexamethasone-inducible promoter (Snyders et al., 1993). Chinese hamster ovary cells (CHO) were grown in Ham's F12 medium with 10% fetal bovine serum and transiently transfected with the cDNA encoding the HERG (4 μg), KvLQT1 and minK (0.8 μg, respectively) or Kv4.3 (3 μg) channels together with the cDNA encoding the CD8 antigen (0.5 μg) by use of lipofectamine (Life Technologies). Before experimental use, cells were incubated with polystyrene microbeads precoated with anti-CD8 antibody (Dynabeads M450; Dynal, Norway). Most of the cells that were beaded also had channel expression (Caballero et al., 2000). Only beaded cells were used for electrophysiological recording.

Solutions and Drugs. A small aliquot of cell suspension was placed in a chamber mounted on the stage of an inverted microscope (TMS; Nikon Co., Tokyo, Japan). After settling to the bottom of the chamber, *Ltk* and CHO cells were superfused with an external solution containing 130 mM NaCl, 4 mM KCl, 1 mM $CaCl_2$, 1 mM $MgCl_2$, 10 mM HEPES, and 10 mM glucose, pH 7.4 with NaOH. Recording pipettes were filled with an "internal" solution containing 80 mM K-aspartate, 42 mM KCl, 10 mM KH_2PO_4, 5 mM MgATP, 3 mM phosphocreatine, 5 mM HEPES, and 5 mM EGTA, pH 7.2 with KOH. In some experiments, the intracellular K^+ concentration ($[K^+]_i$) was lowered to 25% by the equimolar substitution of K-aspartate by Tris-Cl. All the experiments were performed at 24–25°C. Papillary muscles were superfused with a Tyrode's solution containing 125 mM NaCl, 5.4 mM KCl, 1.8 mM $CaCl_2$, 1.05 mM $MgCl_2$, 24 mM $NaHCO_3$, 0.42 mM NaH_2PO_4, and 11 mM glucose. The solution was bubbled with 95% O_2 and 5% CO_2, pH 7.4, and maintained at a temperature of 35 ± 0.5°C. Candesartan (Astra, Hässle, Mölndal, Sweden) and eprosartan (GlaxoSmithKline, Welwyn Garden City, Hertfordshire, UK) as powder were initially dissolved in dimethyl sulfoxide (Sigma Chemical) to yield 0.1 mM stock solutions. Further dilutions were carried out in external solution to obtain the desired final concentration immediately before each experiment. Control solutions contained the same dimethyl sulfoxide concentrations as the test solution.

Recording Techniques. hKv1.5, HERG, and Kv4.3 currents were recorded using the whole-cell configuration of the patch-clamp technique. Under our experimental conditions, hKv1.5 currents remained unaltered for times longer than 60 min. In contrast, viability of transfected CHO cells transiently expressing HERG and Kv4.3 channels is limited to 30 to 40 min; during this time, the amplitude of both currents remained almost unaltered. KvLQT1+minK currents were measured with the perforated nystatin patch configuration to avoid the washout of the intracellular media and the "run-down" of the current (Delpón et al., 1995). Currents were recorded using Axopatch 200B patch clamp amplifiers (Axon Instruments, Foster City, CA). Pipettes were pulled from Narishige (GD1; Narishige Co Ltd., Tokyo, Japan) borosilicate capillary tubes using a programmable patch micropipette puller (P-87; Sutter Instrument Co., Novato, CA) and were heat polished with a microforge (MF-83; Narishige). To ensure voltage-clamp quality, micropipette resistance was kept below 3.5 MΩ when filled with the internal solution and immersed in the external solution. The capacitive transients elicited by symmetrical 10-mV steps were recorded at 50 kHz (filtered at 10 kHz) for subsequent calculation of capacitive surface area, access resistance, and input impedance. Thereafter, capacitance and series

resistance compensation were optimized and ≈80% compensation was usually obtained. Maximum hKv1.5 current amplitudes at +60 mV averaged 1.1 ± 0.1 nA (n = 29) and mean uncompensated access resistance and cell capacitance were 3.2 ± 0.5 MΩ and 10.2 ± 0.9 pF, respectively (n = 22). In CHO cells, cell capacitance averaged 10.5 ± 0.8 pF and the mean uncompensated access resistance was 2.8 ± 0.1 MΩ (n = 20). Maximum HERG, KvLQT1+minK, and Kv4.3 currents averaged 0.16 ± 0.04 nA (n = 10), 2.3 ± 0.3 nA (n = 17) and 2.9 ± 0.6 nA (n = 14), respectively. Thus, under these conditions, no significant voltage errors (<5 mV) caused by series resistance were expected with the electrodes used. Moreover, the low capacitance enabled fast clamp control. The current records were sampled at 3 to 10 times the antialias filter setting and stored on the hard disk of a Hewlett Packard Vectra VL computer for subsequent analysis. Data acquisition and command potentials were controlled by pClamp 6.1 software (Axon Instruments).

Pulse Protocols and Analysis. After control data had been obtained, bath perfusion was switched to drug-containing solution. Thereafter, an equilibration period of 10 min was allowed to elapse before measuring the drug effects. The holding potential was maintained at −80 mV and the cycle time for any protocol was 10 s to avoid accumulation of inactivation and/or block. The protocol to obtain current-voltage relationships consisted of 250 ms (Kv4.3), 500 ms (hKv1.5), 2000 ms (KvLQT1+minK), or 5000 ms (HERG) pulses that were imposed in 10 mV increments between −80 mV and +60 mV. Between −80 and −40 mV, only passive linear leak was observed and least-squares fits to these data were used for passive leak correction. Deactivating hKv1.5, and KvLQT1+minK "tail" currents were recorded on return to −40 mV. Deactivating HERG tail currents were recorded at −60 mV.

The activation curves of HERG, hKv1.5, and KvLQT1+minK currents were constructed by plotting tail current amplitudes elicited as a function of the membrane potential and fitted with a Boltzmann distribution according to the following equation:

$$y = A/\{1 + \exp[(V_h - V_m)/k]\} \quad (1)$$

where A is the amplitude term, V_h is the midpoint of activation, V_m is the test potential, and k represents the slope factor for the activation curve. Under some circumstances, a Boltzmann distribution with two terms was needed to fit the experimental data:

$$y = A_1/\{1 + \exp[(V_{h1} - V_m)/k_1]\} + A_2/\{1 + \exp[(V_{h2} - V_m)/k_2]\} \quad (2)$$

To describe the time course of currents activation upon depolarization, as well as the tail currents upon repolarization, exponential analysis was used as an operational approach, fitting the current traces to an equation of the form:

$$y = C + A_1\exp(-t/\tau_1) + A_2\exp(-t/\tau_2) + \ldots + A_n\exp(-t/\tau_n) \quad (3)$$

where τ_1, τ_2, and τ_n are the system time constants; A_1, A_2, and A_n are the amplitudes of each component of the exponential; and C is the baseline value. The curve-fitting procedure used a nonlinear least-squares (Gauss-Newton) algorithm; results were displayed in linear and semilogarithmic format, together with the difference plot. Goodness of fit was judged by the χ^2 criterion and by inspection for systematic nonrandom trends in the difference plot. Voltage dependence of Kv4.3 and hKv1.5 currents block was determined as follows: leak-corrected current in the presence of drug was normalized to matching control to yield the fractional block at each voltage. The voltage dependence of block was fitted to

$$f = [D]/\{[D] + K_D^* \times \exp(-z\delta FE/RT)\} \quad (4)$$

where z is valence, F is Faraday's constant, R is the gas constant, T is absolute temperature, [D] represents the drug concentration, δ represents the fractional electrical distance (i.e., the fraction of the transmembrane electrical field sensed by a single charge at the receptor site), and K_D^* represents the apparent dissociation constant at the reference potential (0 mV).

Statistical Methods. Data obtained after drug exposure were compared with those obtained under control conditions in a paired manner. For comparisons at a single voltage differences were analyzed using the Student's t test. To analyze block at multiple voltages, two-way analysis of variance was used followed by Newman-Keuls test. Results are expressed as mean ± S.E.M. A P-value of less than 0.05 was considered significant. More details on each procedure are given under *Results*.

Results

Effects of Candesartan and Eprosartan on hKv1.5 Currents. Figure 1, A and B, show hKv1.5 superimposed current traces recorded in two cells when applying 500-ms depolarizations to +60 mV in the absence and presence of 0.1 μM candesartan and 1 μM eprosartan, respectively. Under control conditions, hKv1.5 currents activated with a sigmoidal time course. The currents rose rapidly to a peak and the time constant of activation decreased as the membrane potential became more positive (τ = 1.7 ± 0.1 ms, at +60 mV and τ = 27.4 ± 1.9 ms at −10 mV, n = 20, $P < 0.001$). At positive membrane potentials, the currents displayed slow and partial inactivation as described previously (Snyders et al., 1993). Candesartan and eprosartan decreased the hKv1.5 current amplitude at the end of the pulse by 20.9 ± 2.3% (n = 6, $P < 0.05$) and 14.3 ± 1.5% (n = 8, $P < 0.05$), respectively. It can be observed that candesartan induced an acceleration of the current decline during the depolarizing pulse, whereas eprosartan simply scaled down the current amplitude. C and D show the tail currents elicited on return to −40 mV after the pulses to +60 mV. Both candesartan and eprosartan slowed the tail current deactivation. Thus, candesartan increased the time constant of tail current decline from 48.4 ± 6.7 ms to 67.4 ± 8.5 ms (n = 6, $P < 0.01$), and eprosartan from 63.6 ± 11.6 ms to 149.5 ± 15.0 ms (n = 6, $P < 0.01$). Consequently, in the presence of both drugs, a "crossover" of the tail currents was observed. The effects of both drugs were reversible upon superfusion with drug-free external solution for 7 to 10 min.

In the next group of experiments, we evaluated whether the blockade of hKv1.5 currents increased under conditions of repetitive stimulation. For this purpose, trains of 16 200-ms pulses to +10 or +60 mV were applied. Pulses during the train were applied either every 500 ms or every 1000 ms, and trains were separated from each other by 2-min intervals. Under control conditions, the current amplitude decreased by 7.3 ± 1.1% and 15.8 ± 1.2% (n = 16) when pulses to +10 mV were applied every 500 and 1000 ms, respectively. Figure 1, E and F, show the ratio of current amplitudes in the presence of either candesartan or eprosartan (I_{drug}/I_{con}) as a function of the number of pulse during trains of pulses to +10 mV. The percentages of block obtained from the ratio of current amplitudes in the absence and in the presence of either candesartan or eprosartan during the application of the trains were averaged in Table 1. A certain amount of block was apparent from the first depolarization applied (i.e., "tonic block"). Thereafter, during the train the blockade increased until a steady state was achieved. As can be observed in Fig. 1 and Table 1, both in the presence of candesartan and eprosartan, the blockade was significantly more marked when the interval between pulses was shorter (500 ms). The onset

kinetics of the frequency-dependent block was analyzed by fitting to a monoexponential function the relative current against the number of consecutive pulses of the trains (continuous lines in Fig. 1, E and F). Steady-state frequency dependent block was achieved between the third and fifth pulse of the train and no significant differences in the onset kinetics were observed between both drugs. In fact, the rate constants of the onset kinetics (K) when applying trains of pulses to +10 mV separated by 500-ms interpulse intervals in the presence of candesartan and eprosartan were 0.33 ± 0.08/pulse and 0.29 ± 0.04/pulse, respectively. These results indicated that under conditions of repetitive stimulation, the blockade significantly increased, suggesting that both drugs bind preferentially to an open state of the hKv1.5 channel.

Voltage-Dependent hKv1.5 Block. Fig. 2 shows the current-voltage relationship (I-V) curves obtained in the absence and in the presence of 0.1 μM candesartan (Fig. 2A) or 1 μM eprosartan (Fig. 2B). The I-V curves were obtained by plotting the current amplitude at the end of the depolarizing pulse as a function of the membrane potential. Both candesartan and eprosartan decreased hKv1.5 currents elicited by pulses positive to −30 mV ($P < 0.05$). To quantify the voltage dependence of block in Fig. 2, B and C, the ratio I_{drug}/I_{con} for each group of experiments was plotted as a function of the membrane potential together with the mean activation curve obtained in control conditions. The voltage-dependence displayed a similar pattern for both drugs. The blockade increased in the voltage range coinciding with the activation of the channels, reached a maximum at ≈0 mV and thereafter decreased with a shallow voltage-dependence. In fact, both in the presence of candesartan and eprosartan, the blockade induced at +10 mV (25.5 ± 2.3%, $n = 6$, and 18.3 ± 4.6%, $n = 8$, respectively) was significantly higher than that obtained at +60 mV ($P < 0.05$). The voltage-dependence for channel unblock can be explained if it is considered that both candesartan and eprosartan are weak acids ($pK_a \approx 5.3$), so that at physiological pH, they are present in both the uncharged and the anionic form. Thus, this shallow voltage-dependence can be attributed to the effects of the transmembrane electrical field on the interaction between the anionic form of the drugs and its receptor at the channel level. Fitting the experimental data to a Woodhull formalism (Eq. 4 under *Materials and Methods*) (Woodhull, 1973), the fractional electrical distance ($z\delta$) calculated averaged −0.19 ± 0.05 and −0.18 ± 0.01 in the presence of candesartan and eprosartan, respectively. Further analysis of the voltage-dependence of hKv1.5 chan-

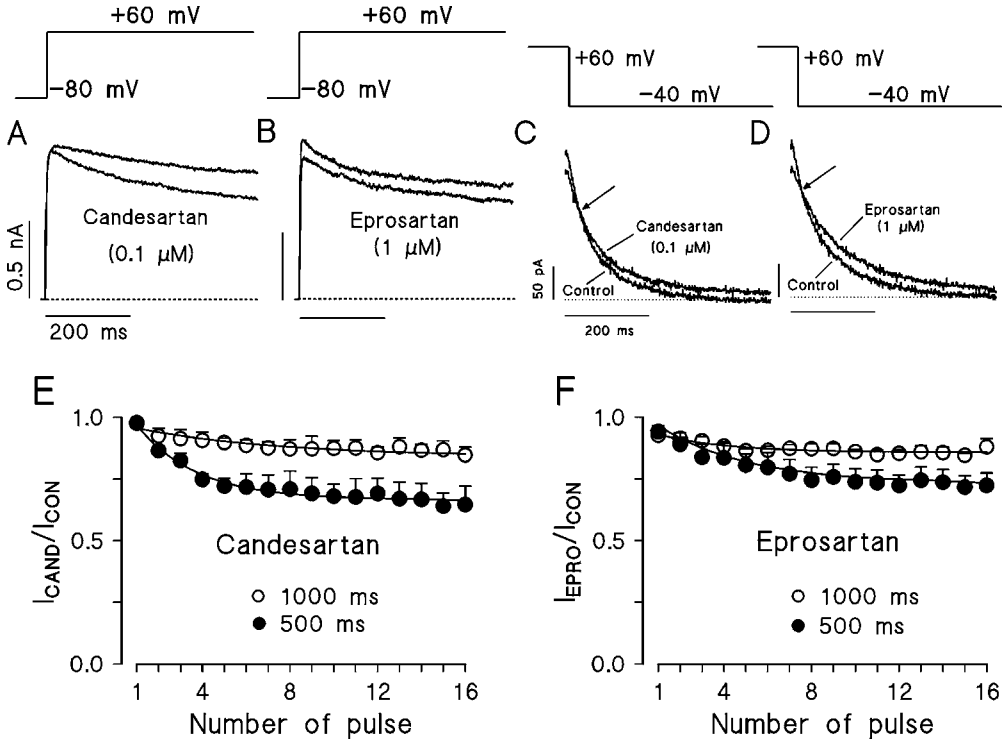

Fig. 1. Effects of candesartan and eprosartan on hKv1.5 currents. A and B, effects of 0.1 μM candesartan and 1 μM eprosartan on hKv1.5 currents recorded in two different cells. Superimposed current traces are shown for 500-ms pulses from −80 mV to +60 mV. C and D, effects of candesartan and eprosartan on the tail currents elicited on return to −40 mV after pulses to +60 mV. The arrows indicate crossover of the tail currents. In A to D, the dotted line represents the zero current level. E and F show the plot of the ratio of the amplitude of the current in the presence and in the absence of candesartan and eprosartan when trains of 200-ms pulses to +10 mV separated by 1000 ms (○) and 500 ms (●) interpulse intervals were applied as a function of the number of pulses. Continuous lines represent the best monoexponential fits of the data. Each data point represents the mean ± SEM of 7 (E) or 10 (F) experiments.

TABLE 1

Frequency-dependent effects induced by candesartan and eprosartan on hKv1.5 currents.

Percentage of tonic and frequency-dependent block induced by 0.1 μM candesartan and 1 μM eprosartan when applying trains of 200-ms depolarizing pulses to +10 or +60 mV. Pulses during the trains were applied at 500 and 1000 ms intervals. Data are mean ± S.E.M. of six to ten experiments.

	+10 mV			+60 mV		
	Tonic Block	Frequency-Dependent Block		Tonic Block	Frequency-Dependent Block	
		1000-ms Interval	500-ms Interval		1000-ms Interval	500-ms Interval
	%					
Candesartan	3.8 ± 1.9	15.2 ± 3.2	35.3 ± 7.5*	5.2 ± 2.3	15.8 ± 3.8	34.6 ± 5.0*
Eprosartan	7.6 ± 0.7	12.5 ± 2.7	25.5 ± 5.6*	6.6 ± 1.9	14.3 ± 3.6	26.2 ± 3.9*

* $P < 0.05$ vs blockade obtained with 1000-ms interpulse intervals.

nel activation revealed that candesartan and eprosartan dramatically modified this process. Figure 2, E and F, show the activation curves in the absence and the presence of drug obtained by plotting the peak tail current amplitude as a function of the membrane potential. Under control conditions, the activation curves were obtained fitting a Boltzmann distribution (Eq. 1 under *Materials and Methods*) to the experimental data and the V_h and k averaged -19.8 ± 1.3 mV and 3.6 ± 0.09 mV ($n = 18$), respectively. However, it can be observed that data obtained in the presence of candesartan or eprosartan clearly deviated from the dashed lines, which represented the fit of the data to a single Boltzmann function and that the activation curve of hKv1.5 channels

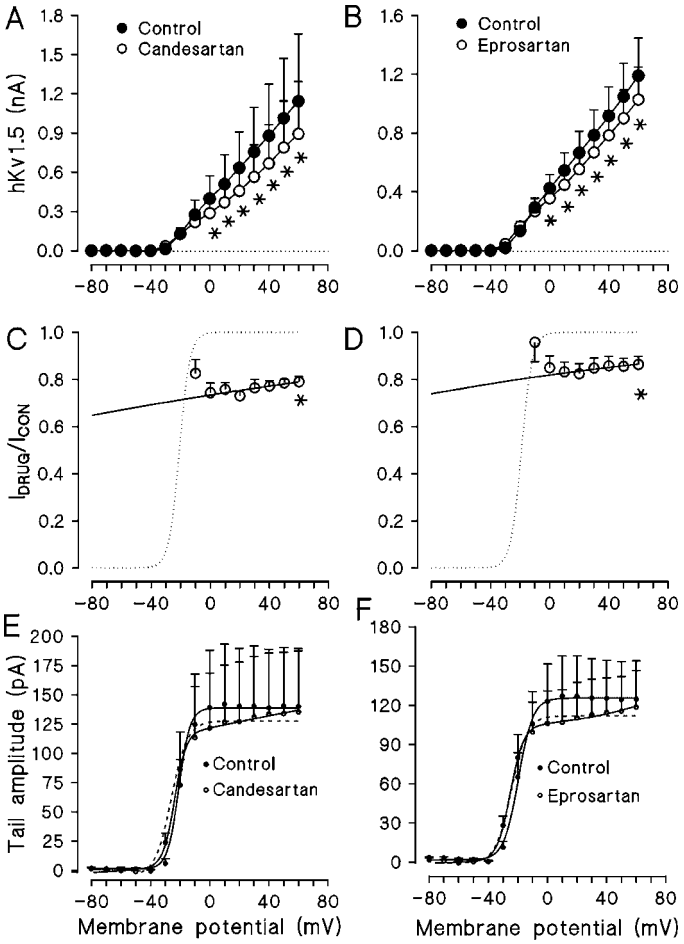

Fig. 2. Voltage-dependent effects of candesartan and eprosartan on hKv1.5 currents. A and B, current voltage relationships (500 ms isochronal) of hKv1.5 channels in the absence and in the presence of candesartan (0.1 μM) or eprosartan (1 μM). The dotted line represents the zero current level. *$P < 0.05$ versus control data. C and D, fractional block ($f = I_{drug}/I_{con}$) from data shown in A and B. The dotted line represents the mean activation curve in control conditions for each group of experiments. The continuous lines represent the best fit to the data positive to 0 mV using the Woodhull formalism (Eq. 4 under *Materials and Methods*) with an apparent equivalent electrical distance of $z\delta = -0.19 \pm 0.05$ and -0.18 ± 0.01 for candesartan and eprosartan, respectively. *$P < 0.05$ versus data at +10 mV. E and F, effects of candesartan or eprosartan on the voltage-dependence of hKv1.5 channel activation. Activation curves in the absence of drugs were fitted with a single Boltzmann component (continuous line, Eq. 1 under *Materials and Methods*), and in the presence of candesartan and eprosartan, they were fitted with a sum of two components (solid line, Eq. 3 under *Materials and Methods*). Dashed lines represent the fit of the data in the presence of drugs with a single Boltzmann component. Each data point represents the mean ± S.E.M. of six to nine experiments.

displayed two components. The first, steeper component was responsible for ≈75% of the activation process and was followed by a shallow component. The solid lines in Fig. 2, E and F, illustrated a fit with a sum of two Boltzmann components (Eq. 2 under *Materials and Methods*) and the averaged values for V_h and k values for each component were summarized in Table 2. Candesartan and eprosartan did not modify the k values but significantly shifted the V_h of the steeper component to potentials that are more negative.

Effects of Candesartan and Eprosartan at Low Intracellular $[K^+]_i$. To elucidate the mechanisms of the voltage-dependent effects of candesartan and eprosartan on hKv1.5 channels, in another group of experiments, the $[K^+]_i$ was decreased to 25% (35 mM). Reduction of the $[K^+]_i$ significantly decreased the maximum outward hKv1.5 current elicited at +60 mV (from 1.1 ± 0.1 nA to 0.6 ± 0.1 nA, $n = 20$, $P < 0.01$) and the peak tail current measured on return to −40 mV (from 136.2 ± 17.9 pA to 55.8 ± 14.0 pA, $n = 20$, $P < 0.01$). Figure 3A shows current traces obtained in the absence and the presence of 0.1 μM candesartan when applying 500-ms pulses to +60 mV. Under these experimental conditions, the candesartan-induced block was significantly reduced compared with that produced at 142 mM $[K^+]_i$ ($6.9 \pm 1.0\%$, $n = 6$, $P < 0.05$). In contrast, Fig. 3B shows that the eprosartan-induced block was similar to that produced at normal $[K^+]_i$ ($17.6 \pm 2.2\%$, $n = 6$, $P > 0.05$). Furthermore, at 35 mM $[K^+]_i$, the time course of tail current deactivation was slowed in the presence of both drugs. Thus, both candesartan ($\tau_{CANDE} = 141.3 \pm 16.5$ ms versus $\tau_{CON} = 75.2 \pm 13.0$ ms, $n = 6$, $P < 0.01$) and eprosartan ($\tau_{EPRO} = 149.5 \pm 15.0$ ms versus $\tau_{CON} = 63.6 \pm 11.6$ ms, $n = 6$, $P < 0.01$) increased the time constant of tail current deactivation. Figure 3, C and D, show the current ratio (I_{drug}/I_{con}) obtained in the presence of candesartan and eprosartan, respectively, as a function of the membrane potential. In both , the dotted line represents the mean activation curve obtained in control conditions in each group of experiments. The reduction of the $[K^+]_i$ suppressed the voltage-dependent unblock produced at potentials positive to 0 mV (see Fig. 2). In fact, the blockade obtained in the presence of candesartan or eprosartan at 0 mV ($6.1 \pm 0.9\%$, $n = 6$ and $20.5 \pm 3.2\%$, $n = 6$, respectively) and + 60 mV was similar. Figure 3, E and F, show the activation curves in the absence and in the presence of either candesartan or eprosartan. Surprisingly, candesartan increased the tail current amplitudes at all the potentials tested, this effect being more marked at negative than at positive potentials. As is shown in Table 2, candesartan and eprosartan did not modify the k values and significantly shifted the V_h to potentials that were more negative ($P < 0.05$), an effect that can account for the increase in current amplitude observed at the membrane potentials at which channel activation occurs. More interestingly, at low $[K^+]_i$ the activation curve of hKv1.5 channels obtained in the presence of both drugs was fitted to a single Boltzmann function (i.e., it did not become biphasic).

Effects of Candesartan and Eprosartan on HERG Currents. HERG encodes the α-subunit of the channel that generates the fast-activating delayed rectifier current (I_{Kr}) in native human cardiac cells (Sanguinetti et al., 1995). Figure 4, A and B, show current traces of HERG currents elicited in transiently transfected CHO cells when applying 5-s pulses to −10 mV from a holding potential of −80 mV, in the absence and presence of 0.1 μM candesartan and 1 μM epro-

sartan. On return to −60 mV, an outward tail current was recorded. The time constant of HERG currents activation at −10 mV was obtained fitting a monoexponential function to the current traces, the resulting time constant of activation averaging 2257 ± 219 ms (n = 14). In contrast, tail current decline was better described by a biexponential function and the fast (τ_f) and slow (τ_s) time constants of deactivation averaged 245 ± 19 and 1309 ± 129 ms, respectively. As shown in Fig. 4A, candesartan increased the maximum outward current elicited at the end of the pulse to ±10 mV, an effect accompanied by an acceleration of the current activation, so that the time constant of activation decreased to 1595 ± 281 ms (n = 7, $P < 0.01$). Moreover, candesartan increased the peak tail current amplitude, whereas it did not modify the time course of tail current deactivation (τ_f = 268 ± 40 ms and τ_s = 1368 ± 156 ms, n = 7, $P > 0.05$). Figure 4C presents the I-V relationship of HERG currents in the absence and the presence of candesartan. At voltages ranging between −40 and 0 mV candesartan significantly increased the current amplitude ($P < 0.05$), whereas, at potentials that were more depolarized, a slight decrease was observed ($P > 0.05$). Figure 4E presents the voltage dependence of HERG channels activation derived from the amplitude of deactivating tail currents recorded on return to −60 mV. The control data were described with a single Boltzmann equation and the values for V_h and k averaged −4.9 ± 2.6 mV and 8.1 ± 0.3 mV, respectively (n = 8). Candesartan shifted the activation curve to more negative potentials (V_h = −14.3 ± 3.3 mV, n = 8, $P < 0.01$), an effect that can account for the increase of the tail current amplitudes observed at potentials between −40 and 0 mV. At potentials that were more positive, however, a decrease of the tail current amplitude was apparent. In Fig. 4E, squares represent the ratio of tail current amplitude in the presence and in the absence of drug. The blockade steeply increased from 0 to +10 mV and thereafter it remained constant (12.9 ± 4.8%, at +60 mV, n = 7, $P > 0.05$). Deactivation kinetics of the tail currents recorded on return to −60 mV after pulses to +60 mV was described by a biexponential function (τ_f = 226 ± 14 ms and τ_s = 1271 ± 83 ms, n = 7) and candesartan did not modify the time course of tail current deactivation.

Figure 4B shows HERG current traces obtained in the absence and the presence of 1 μM eprosartan. Eprosartan also increased the maximum current amplitude, but this effect was not accompanied by an acceleration of the kinetics of current activation (τ = 1952 ± 220 ms, n = 6, $P > 0.05$). The peak tail current amplitude was also increased by eprosartan, but the tail current deactivation kinetics was not modified (τ_f = 275 ± 18 and τ_s = 1521 ± 290 ms, n = 6, $P > 0.05$). The I-V relationship in the absence and the presence of eprosartan is plotted in Fig. 4D. Eprosartan also increased the current amplitude at potentials ranging from −40 to 0 mV, but this effect did not reach statistical significance (n = 6, $P > 0.05$), whereas at more positive potentials, a blocking effect was observed. Fig. 4F represents the voltage-dependence of HERG channel activation in the absence and in the presence of eprosartan. Eprosartan did not modify the V_h (−9.2 ± 3.0 versus −4.6 ± 2.1 mV) or the k values (8.1 ± 0.1 versus 8.0 ± 0.3 mV n = 5, $P > 0.05$) of the activation curve. In addition, eprosartan-induced block increased at potentials coinciding with channel opening and remained constant thereafter. Eprosartan decreased the amplitude of the tail currents elicited on return to −60 mV after 5-s pulses to +60 mV from 239 ± 78 pA to 179 ± 72 pA (n = 5, $P < 0.01$). This effect, however, was not accompanied by a modification of the deactivation kinetics. In fact, the fast and the slow time constants of deactivation in the absence (τ_f = 208 ± 25 ms and τ_s = 1198 ± 161 ms) and presence of eprosartan (τ_f = 207 ± 21 ms and τ_s = 867 ± 121 ms) were not statistically different (n = 5, $P > 0.05$).

Effects of Candesartan and Eprosartan on KvLQT1+minK Currents. Coassembly of KvLQT1 α-subunits with minK β-subunits forms the channels underlying human cardiac I_{Ks} currents (Barhanin et al., 1996; Sanguinetti et al., 1996). Thus, we analyzed the effects of 0.1 μM candesartan and 1 μM eprosartan on KvLQT1+minK currents recorded in CHO cells. Figure 5A shows the I-V relationship obtained by plotting KvLQT1+minK current amplitude at the end of the 2-s pulse as a function of the membrane potential. Maximum outward KvLQT1+minK currents elicited by pulses to +60 mV averaged 2425 ± 380 pA (n = 10). Under whole-cell conditions, KvLQT1+minK currents exhibited a fast (<10 min) and marked (more than 40%) time-dependent decrease. Thus, and to avoid the time-dependent "rundown", KvLQT1+minK currents were recorded using the perforated-nystatin patch configuration of the patch-clamp technique. Figure 5B shows the amplitude of the current recorded at +60 mV in the absence, presence, and after the washout of candesartan. It can be observed that, under these conditions, the amplitude of the currents remained constant for more than 20 min. In the present study, only those experiments in which drug effects were reversible upon washout were included.

Figure 5C shows KvLQT1+minK current traces elicited by applying 2-s pulses from −80 to +60 mV in the absence and presence of candesartan. To describe the dominant time con-

TABLE 2

Effects of candesartan and eprosartan on the voltage dependence of hKv1.5 channel activation.

Values represent the midpoint (V_h) of activation and the slope factor (k) of the activation curves. Data are mean ± S.E.M. of nine experiments.

$[K^+]_i$	Drug	V_{h1}	k_1	V_{h2}	k_2
mM			*mV*		
142	Control	−20.9 ± 1.2	3.5 ± 0.2		
	Candesartan	−24.4 ± 1.9*	3.8 ± 0.2	26.7 ± 4.0	21.9 ± 0.7
	Control	−18.9 ± 2.1	3.7 ± 0.2		
	Eprosartan	−25.5 ± 1.5*	3.6 ± 0.7	21.7 ± 4.2	15.8 ± 1.1
35	Control	−23.9 ± 0.7	3.6 ± 0.3		
	Candesartan	−28.2 ± 0.8*	4.3 ± 0.3*		
	Control	−24.1 ± 0.7	3.7 ± 0.5		
	Eprosartan	−28.6 ± 1.3*	3.4 ± 0.4		

* $P < 0.05$ vs. control.

stants of the activation process of KvLQT1+minK currents, an exponential analysis was used. Fitting KvLQT1+minK traces to +60 mV by a biexponential function, fast (τ_f = 239 ± 36 ms) and slow (τ_s = 1225 ± 206 ms) time constants of activation have been calculated. On return to −40 mV, a deactivating tail current was recorded that declined slowly with monoexponential kinetics (τ = 887 ± 92 ms). Candesartan reduced the maximum outward current amplitude by 38.7 ± 6.3%, (n = 6, $P < 0.05$), but this effect was not accompanied by a modification in the activation kinetics (τ_f = 208 ± 38 ms and τ_s = 1105 ± 313 ms, n = 6, $P > 0.05$). The current ratio between candesartan-sensitive current during the depolarizing pulse and the current in control conditions [$(I_C-I_{CAND})/I_C$] is shown in the upper part of Fig. 5C. The blockade increased during the application of the depolarizing pulse. The onset of block was fitted by a single exponential function, as shown by the solid curve to determine the time constant of development of block which averaged 366 ± 120 ms (n = 6). Candesartan also decreased the peak tail current amplitude without modifying the time course of tail current decline (τ = 885 ± 80 ms, n = 6, $P > 0.05$).

Figure 5D shows the effects of eprosartan on KvLQT1+minK currents in the absence, 3 min after the beginning of drug superfusion, and when the steady-state effect of the drug was reached. At the beginning of the perfusion, eprosartan induced a transient increase in the current amplitude that averaged 8.8 ± 2.7% at the end of the 2-s pulse to +60 mV after 3 min. Thereafter, eprosartan progressively decreased the current amplitude to a steady-state value within ≈10 min (17.7 ± 3.0%, n = 6, $P < 0.05$). Eprosartan did not modify the fast (256 ± 53 versus 312 ± 89 ms) or the slow (1063 ± 151 versus 977 ± 123 ms) time constants of KvLQT1+minK currents activation and, even when it decreased the peak tail current, no change in the time course of current decline was observed (899 ± 68 ms versus 859 ± 52 ms, n = 6, $P > 0.05$).

Effects of Candesartan and Eprosartan on Kv4.3 Currents. Kv4.3 channels are expressed at high levels in human hearts. The functional profile of Kv4.3 channels expressed in mammalian cells closely corresponds to, but did not recapitulate in full detail, the I_{to1} recorded in native cells

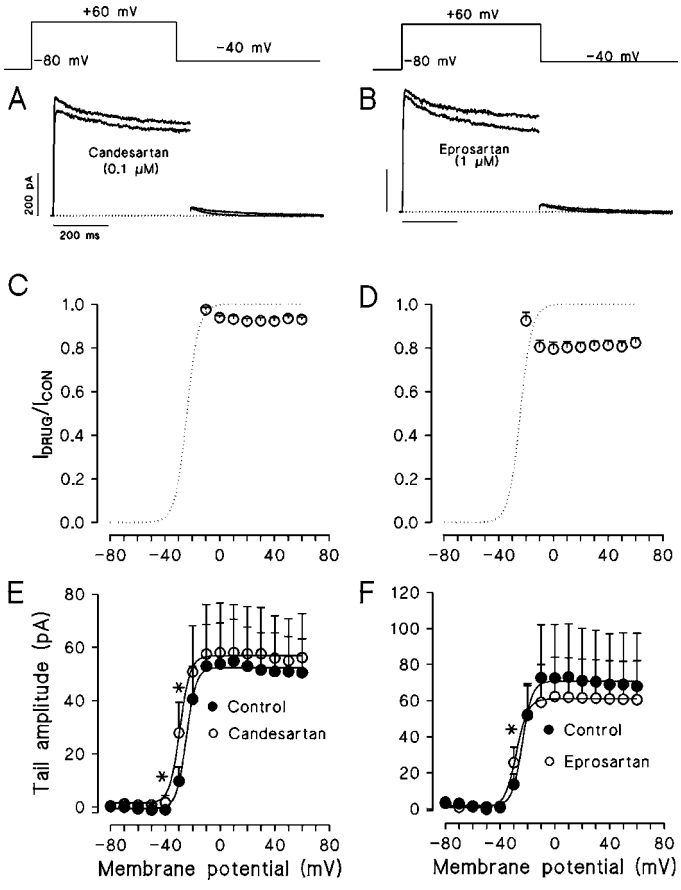

Fig. 3. Effects of candesartan and eprosartan on hKv1.5 channels at low $[K^+]_i$. A and B, superimposed current traces are shown for 500-ms pulses from −80 mV to +60 mV obtained in the absence and in the presence of 0.1 μM candesartan and 1 μM eprosartan, respectively. The dotted line represents the zero current level. C and D, fractional block ($f = I_{drug}/I_{con}$) from data obtained in the presence and in the absence of candesartan and eprosartan, respectively. The dotted line represents the mean activation curve in control conditions for each group of experiments. E and F, effects of candesartan or eprosartan on the voltage-dependence of hKv1.5 channel activation. Activation curve in the absence and in the presence of drugs was fitted with a single Boltzmann component (continuous line, Eq. 1 under *Materials and Methods*). *$P < 0.05$ versus control. Each data point represents the mean ± S.E.M. of six experiments.

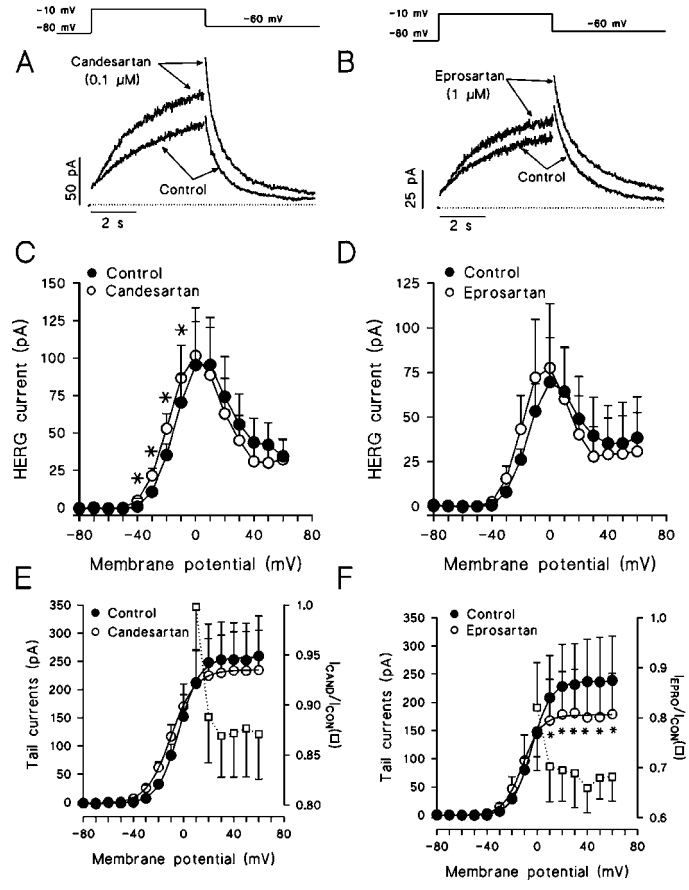

Fig. 4. Effects of candesartan and eprosartan on HERG currents. A and B, effects of 0.1 μM candesartan and 1 μM eprosartan on HERG currents elicited by 5-s pulses from −80 to −10 mV followed by repolarizations to −60 mV. The dotted line represents the zero current level. C and D, I-V relationships (5 s isochronal) of HERG channels recorded in the absence and in the presence of candesartan or eprosartan, respectively. E and F, effects of candesartan or eprosartan on the voltage-dependence of HERG channel activation. Activation curves in the absence and in the presence of drugs were fitted with a single Boltzmann component (continuous line, Eq. 1 under *Materials and Methods*). Squares represent the fractional block ($f = I_{drug}/I_{con}$) from data obtained in the presence and in the absence of candesartan or eprosartan. C and F, *$P < 0.05$ versus control. Each point represents the mean ± S.E.M. of five to eight experiments.

(Dixon et al., 1996). In the present experiments, we studied the effects of 0.1 μM candesartan and 1 μM eprosartan on Kv4.3 channels transiently expressed on CHO cells. Figure 6, A and B, show Kv4.3 current traces elicited in CHO cells when applying 250-ms pulses to +50 mV from a holding potential of −80 mV. Currents rose rapidly to a peak (τ_{act} = 1.3 ± 0.1 ms at +50 mV, n = 20), and then inactivated according to a biexponential process, and τ_f and τ_s averaged 23.3 ± 1.8 ms and 77.1 ± 5.7 ms, respectively (n = 20). Candesartan (Fig. 6A) decreased the peak current elicited at +50 mV by 19.4 ± 2.6% ($n = 7, P > 0.05$) and accelerated the time course of the inactivation process, decreasing the τ_f and τ_s values to 15.1 ± 2.8 ms and 48.1 ± 4.8 ms ($n = 7, P < 0.05$), respectively. Figure 6C represents the I-V relationship obtained by plotting the peak current amplitude as a function of the voltage of the pulse test in the presence and in the absence of candesartan. Squares represent the current ratio (I_{cand}/I_{con}) for membrane potentials positive to 0 mV. Candesartan slightly decreased the peak Kv4.3 current amplitude, an effect that did not reach statistical significance and was voltage-independent. Thus, the most marked effect of candesartan on Kv4.3 channels was an acceleration of current decline, which is suggestive of an open-channel block mechanism, in which case the reduction of peak current would not represent the steady-state block. Therefore, candesartan-induced block was also measured as the reduction in the total charge crossing the membrane estimated from the integral of the current for each test potential. Figure 6E represents the values of charge as a function of the potential of the test pulse in the absence and the presence of candesartan. Candesartan significantly decreased the charge crossing the membrane for test pulses positive to −20 mV ($n = 7, P < 0.05$). In Fig. 6E, squares represent the ratio of charge in the presence and in the absence of candesartan, which was not modified at any of the potentials tested, thus indicating that the decrease in charge induced by candesartan was voltage-independent. Moreover, candesartan decreased the charge crossing the membrane when 250-ms pulses to +50 mV were applied by 36.6 ± 3.6%, an inhibition that was significantly more marked than that produced on the peak current at the same voltage ($P < 0.01$).

Figure 6B shows the effects of eprosartan on Kv4.3 currents. As with candesartan, eprosartan slightly decreased the peak current amplitude elicited by pulses to +50 mV (22.2 ± 3.5%, n = 9, $P < 0.05$). However, it did not significantly modify the time course of current inactivation, so that τ_f and τ_s in the absence and the presence of eprosartan averaged 19.5 ± 1.1 ms and 17.2 ± 2.5 ms ($n = 9, P > 0.05$) and 67.9 ± 8.9 ms and 60.9 ± 6.7 ms ($P > 0.05$), respectively. Figure 6D shows the I-V relationship for Kv4.3 channels in the absence and the presence of eprosartan, together with the current ratio. Eprosartan-induced block was voltage-dependent, so that it reached a maximum at −10 mV (34.9 ± 6.4, n = 9, $P < 0.01$); thereafter, the blockade decreased with a shallow voltage-dependence. Fitting this voltage-dependence to a Woodhull formalism (Eq. 4 under *Materials and Methods*), the fractional electrical distance calculated averaged $z\delta = -0.37 \pm 0.09$ (n = 9). Figure 6F shows the charge/voltage curve in the absence and the presence of eprosartan. Eprosartan significantly reduced the total charge crossing the membrane at all the membrane potentials at which current was activated. However, this decrease was not voltage-dependent. Thus, the ratio of charge in the presence and in the absence of eprosartan (Fig. 6F, □) remains unchanged at all the potentials tested. Moreover, and because eprosartan did not modify the time course of Kv4.3 current inactivation, the eprosartan-induced decrease in charge was not significantly different (29.3 ± 2.8% at +50 mV) from the reduction induced on the peak current.

To further analyze the effects of candesartan and eprosar-

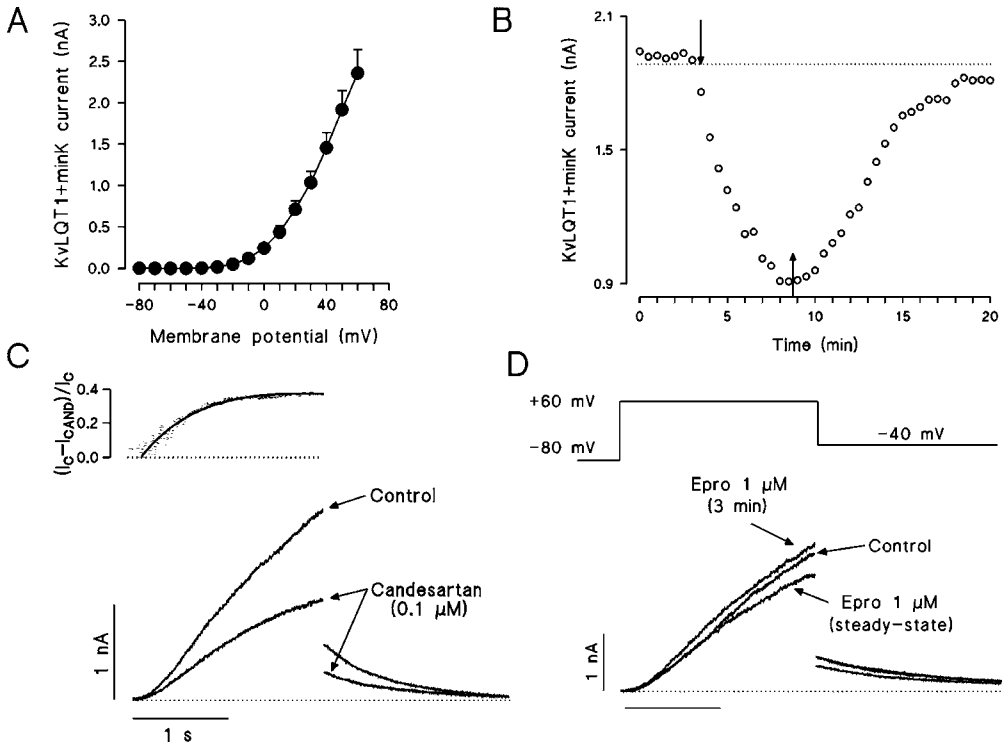

Fig. 5. Effects of candesartan and eprosartan on KvLQT1+minK currents. A, I-V relationships (2 s isochronal) of KvLQT1+minK channels. Each data point represents the mean ± S.E.M. of 10 experiments. B, plot of the KvLQT1+minK current amplitude elicited by 2-s pulses to +60 mV under control conditions, in the presence and after the washout of 0.1 μM candesartan. The arrows indicate the beginning and the end of the superfusion with drug containing solution, respectively. C, effects of candesartan on KvLQT1+minK currents recorded by applying 2-s pulses from −80 mV to +60 mV and upon repolarization to −40 mV. The upper part shows the plot of the current ratio between the candesartan-sensitive current during the depolarizing pulse (I_C-I_{CAND}) and the current in control conditions. An initial value of 0.0 in this plot indicates no block. D, effects of 1 μM eprosartan on KvLQT1+minK currents in the absence, 3 min after the beginning of the drug superfusion and when the steady-state effect of the drug was reached. The dotted line in C and D represents the zero current level.

tan on Kv4.3 channels, the actions of both drugs were studied on the voltage-dependence of inactivation using the double-pulse protocol shown in the upper part of Fig. 7. Figure 7A shows current traces obtained when applying 200-ms pulses to potentials ranging between −90 and +50 mV followed by a test pulse to +40 mV. To construct the inactivation curves, the peak current amplitude elicited by the test pulse was plotted against the membrane potential of the preceding pulse. Under control conditions, the inactivation curve was well described by a Boltzmann function and the V_h and the k values averaged −38.1 ± 2.4 mV and 5.7 ± 0.2 mV (n = 13), respectively. In the presence of candesartan (Fig. 7B), the peak Kv4.3 current decreased, but the V_h and the k values were not modified (−40.2 ± 2.9 mV and 5.7 ± 0.2 mV, n = 7, $P > 0.05$) as it is shown by the curve scaled to the control amplitude (dashed line). Figure 7C shows that eprosartan did not modify the V_h (−33.6 ± 2.9 mV versus −34.1 ± 2.0 mV, n = 6, $P > 0.05$) and the k values (5.7 ± 0.1 versus 5.9 ± 0.3 mV, $P > 0.05$) of the inactivation curve.

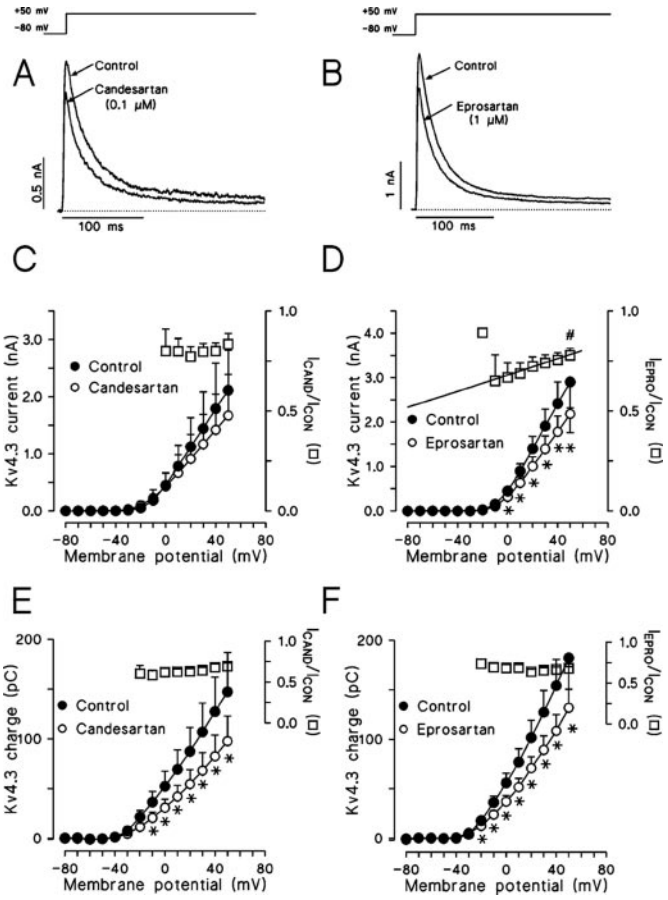

Fig. 6. Effects of candesartan and eprosartan on Kv4.3 currents. A and B, superimposed Kv4.3 currents elicited by 250-ms pulses from −80 to +60 mV in the absence and in the presence of 0.1 μM candesartan and 1 μM eprosartan, respectively. C and D, I-V relationship for peak Kv4.3 currents in the absence and in the presence of candesartan and eprosartan, respectively. *$P < 0.05$ versus control. □, fractional block ($f = I_{drug}/I_{con}$) from data obtained in the presence and in the absence of each drug. In D, the continuous line represents the best fit to the data positive to −10 mV using the Woodhull formalism (Eq. 4 under *Materials and Methods*) with an apparent equivalent electrical distance $z\delta = -0.37 \pm 0.09$. #$P < 0.05$ versus data at −10 mV. E and F, relationship between current-time integral and membrane potential in the absence and in the presence of candesartan and eprosartan. *$P < 0.05$ versus control. □, fractional block ($f = I_{drug}/I_{con}$) from data obtained in the presence and in the absence of each drug. Each data point represents the mean ± S.E.M. of seven to nine experiments.

Effects of Candesartan and Eprosartan on Ventricular Action Potential Duration. The previous results indicated that candesartan preferentially blocks KvLQT1+minK, whereas eprosartan preferentially blocks HERG channels. Thus, we compared their effects on the characteristics of the ventricular action potentials recorded in guinea pig papillary muscles using conventional microelectrode techniques. Figure 8A shows superimposed action potentials recorded in muscles driven at 1 and 2 Hz in the absence and presence of candesartan and eprosartan. In 12 muscles driven at 1 Hz, the resting membrane potential and the action potential amplitude averaged −85.5 ± 1.7 mV and 126.8 ± 1.1 mV, respectively. Neither candesartan nor eprosartan modified these parameters. Figure 8B shows the action potential duration (APD) measured at 50% (circles) and 90% (squares) of repolarization in the absence and the presence of 0.1 μM candesartan in muscles driven at 0.1, 1, 2, and 3 Hz. Candesartan slightly prolonged the APD at all the frequencies tested, but this effect did not reach statistical significance. Figure 8B shows that the effects of 1 μM eprosartan on the APD were quite different. Eprosartan prolonged the APD in muscles driven at 0.1 and 1 Hz, whereas at faster driving rates, it slightly decreased the ventricular APD, (i.e., eprosartan exhibited "reverse use-dependent" effects on ventricular repolarization) (Hondeghem and Snyders, 1990).

Discussion

In the present study, we have analyzed the effects of candesartan and eprosartan, two specific AT_1 receptor antagonists, on several K^+ currents involved in human cardiac repolarization. Maximum plasma concentrations obtained after administration of therapeutic doses of candesartan (8 to

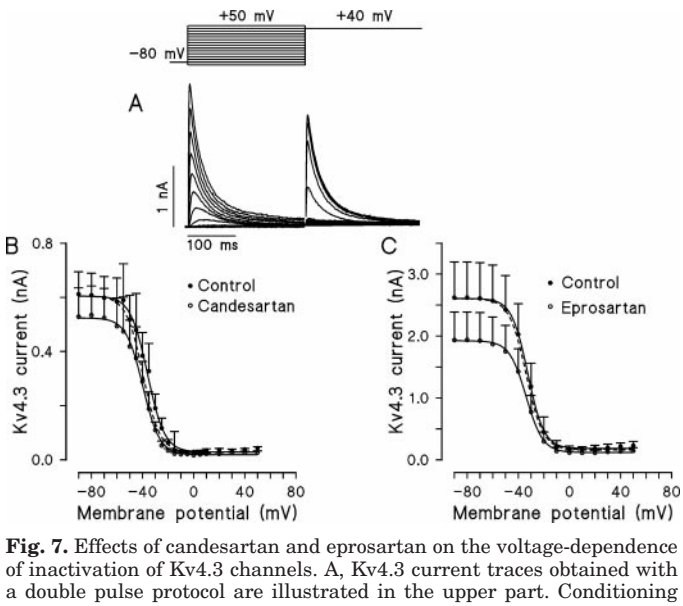

Fig. 7. Effects of candesartan and eprosartan on the voltage-dependence of inactivation of Kv4.3 channels. A, Kv4.3 current traces obtained with a double pulse protocol are illustrated in the upper part. Conditioning pulses from a holding potential of −80 mV were applied to potentials ranging from −90 to +50 mV followed by a 250-ms pulse to +40 mV. B and C, effects of 0.1 μM candesartan and 1 μM eprosartan on the voltage-dependence of Kv4.3 channels inactivation obtained by plotting the peak outward current at +40 mV as a function of the membrane potential of conditioning pulse. Continuous lines represent the best fit to the data using a Boltzmann equation. Dashed lines represent the fit to the data obtained in the presence of drug scaled to the control values. Each data point represents the mean ± S.E.M. of seven to nine experiments.

16 mg/day) or eprosartan (200 to 800 mg/day) were 0.125 to 0.240 μM and 1.7 to 4.4 μM, respectively (McClellan and Balfour, 1998; McClellan and Goa, 1998). Taking into account the marked plasma protein binding of these drugs (≈98%), the expected free plasma concentrations would be about 2 orders of magnitude lower (Burnier and Brunner, 2000). Thus, the present study demonstrated that at concentrations higher than the plasma free concentrations, candesartan and eprosartan exert direct effects on hKv1.5, HERG, KvLQT1+minK, and Kv4.3 currents that underlie I_{Kur}, I_{Kr}, I_{Ks}, and I_{to1}, respectively, in human cardiac myocytes. It is important to note that the present experiments were performed in the absence of angiotensin. Moreover, even when the concentrations tested for each drug can be considered equipotent for AT_1 receptor antagonism, the effects of candesartan and eprosartan on each current differ in efficacy and in voltage and time-dependence, which is not consistent with a common mechanism of action (i.e., the blockade of AT_1 receptors).

Effects on hKv1.5 Channels. Blocking effects of candesartan and eprosartan on hKv1.5 channels were moderate, but they increased markedly under conditions of repetitive stimulation. Moreover, both drugs slowed the time course of tail current decline, thus inducing a "crossover phenomenon". The frequency-dependent block and the crossover of the tail currents are compatible with an open-channel block mechanism. Candesartan accelerated the current decline during the depolarizing pulse, whereas eprosartan scaled down the current amplitude. If candesartan bound to the open state and a first-order reaction between the drug molecule and the receptor occurred at the channel level, the time-dependent decline would represent the time course of relaxation toward a new equilibrium. From this point of view, the effects of eprosartan can be explained considering that the development of block is faster than that of candesartan and even than the time-dependent current activation. In addition, candesartan- and eprosartan-induced blockade appeared at the voltage range at which channel opening proceeds; thereafter, it decreased with a shallow voltage-dependence. Simultaneously, both drugs dramatically modified voltage-dependence of hKv1.5 channel activation, so that the activation curves became biphasic. Several hypotheses can account for these effects. First, and considering the gating scheme proposed for hKv1.5 channels ($C \rightleftarrows C \rightleftarrows \ldots \rightleftarrows C \rightleftarrows O_1 \rightleftarrows O_2 \rightleftarrows I_1 \rightleftarrows I_2$) (Rich and Snyders, 1998), the voltage-dependent effects of both drugs can be explained by a fast selective block of the first open state of the channel (O_1) followed by a very fast unblock from the second open state (O_2), which appeared at more positive potentials. Second, candesartan and eprosartan are weak acids ($pK_a \approx 5.3$); at physiological pH, they would predominate in their anionic form. Thus, it is possible that the anionic form of these drugs binds to a receptor located at the intracellular mouth of the pore as it has been demonstrated for quinidine (Snyders et al., 1992) and bupivacaine (Franqueza et al., 1997). From this point of view, the voltage-dependent unblock can be explained considering that the anionic form of both drugs reaches this receptor site from the inside by crossing ≈20% of the membrane electrical field. Another possibility is that the binding site for candesartan and eprosartan is located in the external mouth of the pore in such a way that outward K^+ efflux hinders the binding of drug to its external receptor site with a resultant relief of block. To assess this possibility the $[K^+]_i$ was reduced to 25%. Under these conditions, the voltage-dependent unblock induced by candesartan and eprosartan was abolished. Moreover, the activation curve of hKv1.5 channels did not exhibit two components, and only the shift of the curve to more negative potentials was apparent. These results suggest that the shallow component that appeared at normal $[K^+]_i$ was caused by the unblock produced by the K^+ efflux at positive potentials, which confirmed and extended previous evidence indicating the existence of an external binding site on hKv1.5 channels (Zhang et al., 1997; Caballero et al., 1999; Delpón et al., 1999; Longobardo et al., 2000).

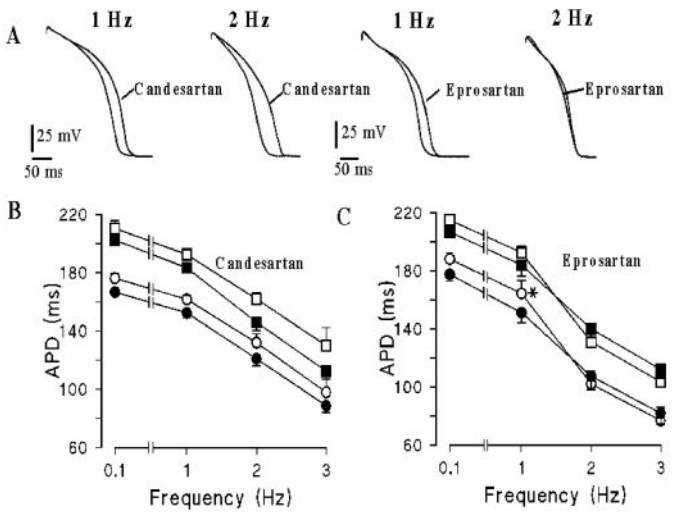

Fig. 8. Effects of candesartan and eprosartan on action potentials recorded in guinea pig papillary muscles driven at 1 and 2 Hz. A, superimposed action potentials recorded in the absence and in the presence of candesartan and eprosartan under these experimental conditions. B and C, the action potential duration measured at 50% (circles) and 90% (squares) of repolarization in the absence (closed symbols) and in the presence (open symbols) of 0.1 μM candesartan and 1 μM eprosartan in muscles driven at 0.1, 1, 2, and 3 Hz, respectively. Each data point represents the mean ± S.E.M. of six experiments. $^*P < 0.05$ versus control.

Effects on HERG and KvLQT1+minK Channels. Both candesartan and eprosartan increased HERG current amplitudes at potentials ranging from −40 to 0 mV, candesartan being more potent for this effect. In addition, eprosartan, but not candesartan, significantly decreased peak tail currents elicited on repolarization after pulses to potentials positive to 0 mV. Furthermore, the eprosartan-induced block steeply increased at voltage range of channel opening, suggesting that it preferentially blocks the open state of HERG channels. Candesartan also modified the *gating* properties of HERG channels, shifting the midpoint of the activation curve toward potentials that were more negative, an effect that can account for the increase in HERG currents. Similar results have been previously described with losartan and E3174 (Caballero et al., 2000), almokalant (Carmeliet, 1993), and azimilide (Jiang et al., 1999). In all cases, the increase in HERG current amplitude ("agonist effect") was best seen at low-voltage depolarizations close to the activation threshold (≈−40 mV). Moreover, the azimilide-induced agonist effect was produced by depolarization pulses in a use-dependent manner, exerted from outside the cell membrane, and seemed to be caused by a modification of the activation-gating process of the HERG channel (Jiang et al., 1999). The

"agonist" effects induced by candesartan and eprosartan were not evaluated under conditions of repetitive stimulation; thus, we cannot rule out the possibility of a use-dependent increase of HERG currents in the presence of both drugs. Moreover, it is possible that the moderate shortening of the APD produced by eprosartan at fast driving rates could be the consequence of such an effect.

The effects of candesartan and eprosartan on KvLQT1+minK channels are opposite those produced on HERG channels. Candesartan markedly inhibited, whereas eprosartan slightly decreased, KvLQT1+minK currents. Because of the rapid rundown of KvLQT1+minK currents, we did not attempt to analyze the voltage-dependence of candesartan-induced block. However, the fast development of block with no block at the beginning of depolarizing pulses strongly suggests an open state interaction.

Effects on Kv4.3. Candesartan slightly decreased the peak current and significantly accelerated the time course of current inactivation, which suggests that it binds to and blocks the pore only when the channel opens. Consequently, candesartan significantly decreases the charge crossing the membrane because of the efflux of K^+ through Kv4.3 channels. However, candesartan-induced block remained constant at the membrane potential range at which channel activation occurs. Assuming that the binding site is located in the pore, this result suggests that the active form of candesartan is the neutral one and/or that the anionic form does not cross the electrical field to reach its binding site. On the other hand, as observed on hKv1.5 channels, eprosartan-induced block of Kv4.3 channels was voltage-dependent. It reached a maximum at −10 mV and significantly decreased at more depolarized potentials. Moreover, in contrast to candesartan, eprosartan did not modify the time course of current inactivation, a result that did not exclude an open-state interaction for eprosartan. Furthermore, candesartan and eprosartan did not modify the voltage-dependence of Kv4.3 channel inactivation, suggesting that they did not bind to the inactivated state of the channel.

Effects on Cardiac Repolarization. Specific I_{Kr} blockers lengthen cardiac APD, but this effect is more pronounced at slow than at fast driving rates, a property known as "reverse use-dependence" (Hondeghem and Snyders, 1990). This property limits their efficacy in terminating tachyarrhythmias and maximizes the risk for development of bradycardia-induced polymorphic ventricular tachyarrhythmias (Tamargo, 2000). On the contrary, it has been proposed that APD prolongation produced by selective I_{Ks} blockers shows less reverse use-dependence (Nattel, 1999). Our results demonstrate that eprosartan preferentially blocks HERG channels, whereas candesartan preferentially blocks KvLQT1+minK channels. Thus, the effects of both drugs on APD were studied in guinea pig papillary muscles, because in this animal species, I_{Kr} and I_{Ks} are the main K^+ currents responsible for repolarization (Sanguinetti and Jurkiewicz, 1990). The present results confirm previous observations that preferential block of I_{Kr} or I_{Ks} produces different effects on APD (Nattel, 1999; Varró et al., 2000). Candesartan slightly prolonged the APD (≈12%) at all the frequencies tested, but this prolongation did not reach statistical significance. This result can be explained because I_{Ks} plays little role during normal action potential repolarization (Varró et al., 2000) and, in addition, candesartan increases HERG currents, an effect that can partially overcome the lengthening caused by I_{Ks} blockade. On the contrary, eprosartan prolongs the APD in muscles driven at slow (0.1 Hz) and normal (1 Hz) heart rates, which confirms that I_{Kr} plays a crucial role in action potential repolarization. However, as described for other I_{Kr} blockers, this lengthening disappeared at fast driving rates (2 and 3 Hz). Further studies are needed to evaluate whether the effects described with candesartan and eprosartan result in a modification of the human cardiac action potential repolarization, a significant undertaking that goes beyond the scope of the present manuscript.

Acknowledgments

We thank Drs. M. M. Tamkun and D. J. Snyders for providing hKv1.5 and Kv4.3 channels and Drs. M Keating and M Sanguinetti for providing the HERG and KvLQT1+minK clones. We also thank Guadalupe Pablo and José Luis Llorente for their technical assistance.

References

Abbott G, Sesti F, Splawski I, Buck M, Lehmann M, Timothy K, Keating M and Goldstein S (1999) MiRP1 forms I_{Kr} potassium channels with HERG and is associated with cardiac arrhythmia. *Cell* **97:**175–187.

Barhanin J, Lesage F, Guillemare E, Fink M, Lazdunski M and Romey G (1996) KvLQT1 and IsK (minK) proteins associate to form the I_{Ks} cardiac potassium current. *Nature (Lond)* **384:**78–80.

Burnier M and Brunner H (2000) Angiotensin II receptor antagonists. *Lancet* **355:** 637–645.

Caballero R, Delpón E, Valenzuela C, Longobardo M and Tamargo J (2000) Losartan and its metabolite E3174, modify cardiac delayed rectifier K^+ currents. *Circulation* **101:**1199–1205.

Caballero R, Valenzuela C, Longobardo M, Tamargo J and Delpón E (1999) Effects of rupatadine, a new dual antagonist of histamine and platelet-activating factor receptors, on human cardiac Kv1.5 channels. *Br J Pharmacol* **128:**1071–1081.

Carmeliet E (1993) Use-dependent block and use-dependent unblock of the delayed rectifier K^+ current by almokalant in rabbit ventricular myocytes. *Circ Res* **73:** 857–868.

Delpón E, Caballero R, Valenzuela C, Longobardo M, Snyders D and Tamargo J (1999) Benzocaine enhances and inhibits the K^+ current through a human cardiac cloned channel (Kv1.5). *Cardiovasc Res* **42:**510–520.

Delpón E, Valenzuela C, Pérez O, Casis O and Tamargo J (1995) Propafenone preferentially blocks the rapidly activating component of delayed rectifier K^+ current in guinea pig ventricular myocytes. Voltage-independent and time-dependent block of the slowly activating component. *Circ Res* **76:**223–235.

Dixon JE, Shi W, Wang HS, McDonald C, Yu H, Wymore RS, Cohen IS and McKinnon D (1996) The role of Kv4.3 K^+ channel in ventricular muscle. A molecular correlate for the transient outward current. *Circ Res* **79:**659–668.

Franqueza L, Longobardo M, Vicente J, Delpón E, Tamkun M, Tamargo J, Snyders D and Valenzuela C (1997) Molecular determinants of stereoselective bupivacaine block of hKv1.5 channels. *Circ Res* **81:**1053–1064.

Habuchi Y, Lu L, Morikawa J and Yoshimura M (1995) Angiotensin II inhibition of L-type Ca^{2+} current in sinoatrial node cells of rabbits. *Am J Physiol* **268:**H1053–H1060.

Harada K, Komuro I, Hayashi D, Sugaya T, Murakami K and Yazaki Y (1998) Angiotensin II type 1a receptor is involved in the occurrence of reperfusion arrhythmias. *Circulation* **97:**315–317.

Hondeghem L and Snyders D (1990) Class III antiarrhythmic agents have a lot of potential, but a long way to go: Reduced effectiveness and dangers of reverse use-dependence. *Circulation* **81:**686–690.

Hubner R, Hogemann A, Sunzel M and Ridell J (1997) Pharmacokinetics of candesartan after single and repeated doses of candesartan cilexetil in young and elderly healthy volunteers. *J Human Hypertens* **11:**S19–S25.

Jiang M, Dun W, Fan J and Tseng G (1999) Use-dependent "agonist" effect of azimilide on the HERG channel. *J Pharmacol Exp Ther* **291:**1324–1336.

Longobardo M, González T, Navarro-Polanco R, Caballero R, Delpón E, Tamargo J and Valenzuela C (2000) Effects of quaternary bupivacaine derivative on delayed rectifier K^+ currents. *Br J Pharmacol* **130:**391–401.

McClellan K and Balfour J (1998) Eprosartan. *Drugs* **55:**713–718.

McClellan K and Goa K (1998) Candesartan cilexetil. A review of its use in essential hypertension. *Drugs* **56:**847–869.

Nakashima H, Kumagai K, Urata H, Gondo N, Ideishi M and Arakawa K (2000) Angiotensin II antagonist prevents electrical remodeling in atrial fibrillation. *Circulation* **101:**2612–2617.

Nattel S (1999) The molecular and ionic specificity of antiarrhythmic drug actions. *J Cardiovasc Electrophysiol* **10:**272–282.

Pérez O, Valenzuela C, Delpón E and Tamargo J (1997) Electrophysiological effects of CI-980, a tubulin binding agent, on guinea-pig papillary muscles. *Br J Pharmacol* **120:**187–192.

Rich T and Snyders D (1998) Evidence for multiple open and inactivated states of the hKv1.5 delayed rectifier. *Biophys J* **75:**183–195.

Roden D and George A (1997) Structure and function of cardiac sodium and potassium channels. *Am J Physiol* **273:**H511–H525.

Sanguinetti M, Curran M, Zou A, Shen J, Spector P, Atkinson D and Keating M

(1996) Coassembly of KvLQT1 and minK (IsK) proteins to form cardiac I_{Ks} potassium channel. *Nature (Lond)* **384:**80–83.
Sanguinetti M, Jiang C, Curran M and Keating M (1995) A mechanistic link between an inherited and an acquired cardiac arrhythmia: HERG encodes the I_{Kr} potassium channel. *Cell* **81:**299–307.
Sanguinetti M and Jurkiewicz N (1990) Two components of cardiac delayed rectifier K^+ current. *J Gen Physiol* **96:**195–215.
Sever P and Holzgreve H (1997) Long-term efficacy and tolerability of candesartan cilexetil in patients with mild to moderate hypertension. *J Hum Hypertens* **11:** S69–S73.
Snyders D, Knoth K, Roberds S and Tamkun M (1992) Time-, state- and voltage-dependent block by quinidine of a cloned human cardiac channel. *Mol Pharmacol* **41:**332–339.
Snyders D, Tamkun M and Bennett P (1993) A rapidly activating and slowly inactivating potassium channel cloned from human heart. Functional analysis after stable mammalian cell culture expression. *J Gen Physiol* **101:**513–543.
Tamargo J (2000) Drug-induced torsade de pointes: From molecular biology to bedside. *Jpn J Pharmacol* **83:**1–19.
Tamkun M, Knoth K, Walbridge J, Kroemer H Roden D and Glover D (1991) Molecular cloning and characterization of two voltage-gated K^+ channel cDNAs from human ventricle. *FASEB J* **5:**331–337.
Timmermans PB, Wong PC, Chiu AT, Herblin WF, Benfield P, Carini DJ, Lee RJ, Wexler RR, Saye AJ and Smith RD (1993) Angiotensin II receptors and angiotensin II receptor antagonists. *Pharmacol Rev* **45:**206–251.
Unger T (1999) Significance of angiotensin type 1 receptor blockade: Why are angiotensin II receptor blockers different? *Am J Cardiol* **84:**9S–15S.
Varró A, Baláti B, Iost N, Takács J, Virág L, Lathrop D, Csaba L, Tálosi L and Papp J (2000) The role of the delayed rectifier component I_{Ks} in dog ventricular muscle and Purkinje fibre repolarization. *J Physiol* **523:**67–81.
Wang Z, Fermini B and Nattel S (1993) Sustained depolarization-induced outward current in human atrial myocytes: Evidence for a novel delayed rectifier K^+ current similar to Kv1.5 cloned channels currents. *Circ Res* **73:**1061–1076.
Wang Z, Feng J, Shi H, Pond A, Nerbonne J and Nattel S (1999) The potential molecular basis of different physiological properties of transient outward K^+ current in rabbit and human atrial myocytes. *Circ Res* **84:**551–561.
Woodhull AM (1973) Ionic blockage of sodium channels in nerve. *J Gen Physiol* **61:**687–708.
Zhang X, Anderson J and Fedida D (1997) Characterization of nifedipine block of the human heart delayed rectifier, hKv1.5. *J Pharmacol Exp Ther* **281:**1247–1256.

Send reprint requests to: Eva Delpón, BPharm, Ph.D., Department of Pharmacology, School of Medicine, Universidad Complutense, 28040-Madrid, Spain. E-mail: edelpon@eucmax.sim.ucm.es